

# IHG-1 Promotes Mitochondrial Biogenesis by Stabilizing PGC-1 $\alpha$

Fionnuala B. Hickey,<sup>\*†</sup> James B. Corcoran,<sup>\*†</sup> Neil G. Docherty,<sup>‡</sup> Brenda Griffin,<sup>\*§</sup>  
Una Bhreathnach,<sup>\*†</sup> Fiona Furlong,<sup>†</sup> Finian Martin,<sup>\*§</sup> Catherine Godson,<sup>\*†</sup>  
and Madeline Murphy,<sup>\*†</sup>

<sup>\*</sup>UCD Diabetes Research Centre, UCD Conway Institute, <sup>†</sup>UCD School of Medicine and Medical Sciences, and

<sup>§</sup>UCD School of Biomolecular and Biomedical Science, University College Dublin, Belfield, Dublin, Ireland; and

<sup>‡</sup>Department of Physiology, Trinity College Dublin, Dublin, Ireland

## ABSTRACT

Increased expression of Induced-by-High-Glucose 1 (IHG-1) associates with tubulointerstitial fibrosis in diabetic nephropathy. IHG-1 amplifies TGF- $\beta$ 1 signaling, but the functions of this highly-conserved protein are not well understood. IHG-1 contains a putative mitochondrial-localization domain, and here we report that IHG-1 is specifically localized to mitochondria. IHG-1 overexpression increased mitochondrial mass and stabilized peroxisome proliferator-activated receptor  $\gamma$  coactivator-1 $\alpha$  (PGC-1 $\alpha$ ). Conversely, inhibition of IHG-1 expression decreased mitochondrial mass, downregulated mitochondrial proteins, and PGC-1 $\alpha$ -regulated transcription factors, including nuclear respiratory factor 1 and mitochondrial transcription factor A (TFAM), and reduced activity of the TFAM promoter. In the unilateral ureteral obstruction model, we observed higher PGC-1 $\alpha$  protein expression and IHG-1 levels with fibrosis. In a gene-expression database, we noted that renal biopsies of human diabetic nephropathy demonstrated higher expression of genes encoding key mitochondrial proteins, including cytochrome c and manganese superoxide dismutase, compared with control biopsies. In summary, these data suggest that IHG-1 increases mitochondrial biogenesis by promoting PGC-1 $\alpha$ -dependent processes, potentially contributing to the pathogenesis of renal fibrosis.

*J Am Soc Nephrol* 22: 1475–1485, 2011. doi: 10.1681/ASN.2010111154

Tubulointerstitial fibrosis (TIF) is the final pathway leading to end-stage renal disease (ESRD) in many chronic kidney diseases.<sup>1,2</sup> Increased expression of the highly conserved transcript induced in high glucose-1 (IHG-1/THG1L/ICF45) is associated with TIF in both diabetic nephropathy (DN) in humans and in experimental renal fibrosis.<sup>3,4</sup> TGF- $\beta$ 1 is a key mediator of TIF.<sup>5,6</sup> IHG-1 overexpression has also been shown to enhance signaling downstream of TGF- $\beta$ 1.<sup>4</sup> As such, we proposed that IHG-1 contributes to the development of TIF. IHG-1 encodes a highly evolutionarily conserved transcript. To date, a mitochondrial localization sequence is the only functional domain identified in IHG-1.

Mitochondrial biogenesis is a complex, highly controlled process requiring coordinated regulation of nuclear and mitochondrial gene expression.<sup>7,8</sup> Peroxisome proliferator-activated receptor  $\gamma$  coactivator-1 $\alpha$  (PGC-

1 $\alpha$ ) acts as a key regulator of mitochondrial biogenesis in mammals.<sup>9–13</sup> PGC-1 $\alpha$  regulates several transcription factors including nuclear respiratory factors (NRF-1 and NRF-2/GABP),<sup>14–16</sup> which have been shown to activate the transcription of a large number of nuclear encoded mitochondrial genes.<sup>17</sup> PGC-1 $\alpha$  enhances expression of NRF-1 and NRF-2 and also increases the transcriptional activity of NRF-1 on the mitochondrial transcription fac-

Received November 12, 2010. Accepted March 29, 2011.

Published online ahead of print. Publication date available at www.jasn.org.

**Correspondence:** Catherine Godson, UCD Conway Institute, School of Medicine and Medical Sciences, University College Dublin, Belfield, Dublin 4, Ireland. Phone: 353-1-716-6731; Fax: 353-1-716-6701; E-mail: catherine.godson@ucd.ie

Copyright © 2011 by the American Society of Nephrology

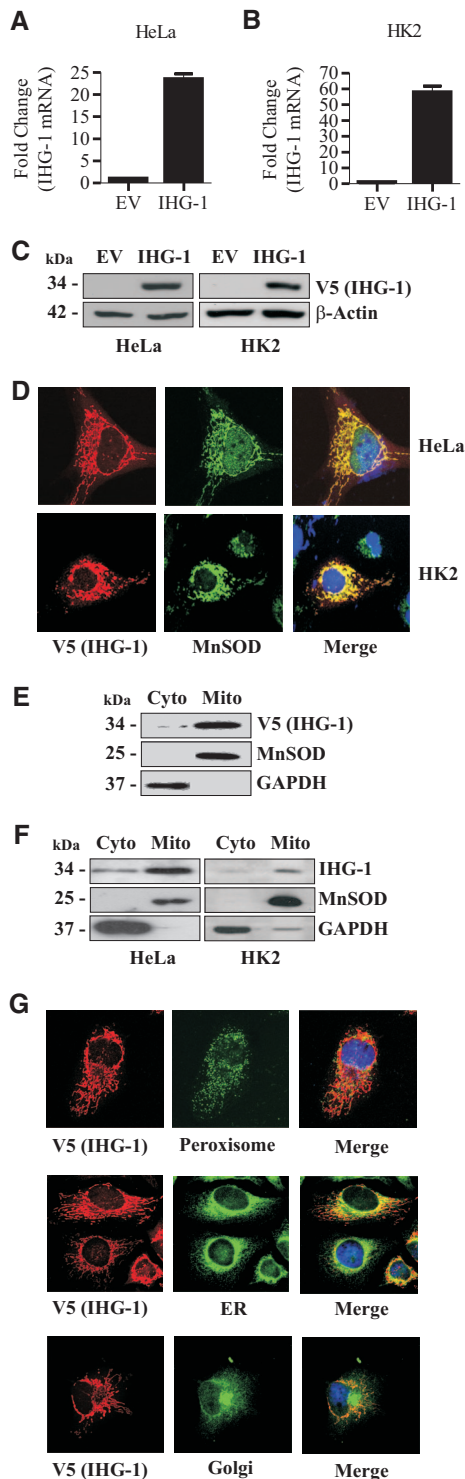


**Figure 1.** Induced-by-High-Glucose 1 (IHG-1) is localized to the mitochondria. (A) Total cellular RNA was prepared from HeLa cells stably overexpressing IHG-1. IHG-1 mRNA was quantified by real-time PCR. The results were normalized to 18 S rRNA and are expressed as relative quantification versus cells transduced with an empty vector (EV). (B) Total cellular RNA was prepared from HK2 cells stably overexpressing IHG-1. IHG-1 mRNA was quantified as in A. (C) Whole-cell lysates from cells in A and B were

analyzed by immunoblotting with antibodies specific for V5. (D) HeLa and HK2 cells expressing IHG-1-V5 were stained with Texas Red-labeled anti-V5 and FITC-labeled anti-manganese superoxide dismutase (MnSOD) and visualized by confocal microscopy. (E) Cytoplasmic (Cyto) and mitochondrial (Mito) extracts prepared from cells in A were analyzed by immunoblotting with antibodies specific for V5. MnSOD and glyceraldehyde-3-phosphate dehydrogenase (GAPDH) were used as markers for mitochondria and cytosol, respectively. (F) Cytoplasmic and mitochondrial protein cell extracts were prepared from HeLa and HK2 cells and were analyzed by immunoblotting with antibodies specific for endogenous IHG-1, MnSOD, and GAPDH. (G) HeLa cells expressing IHG-1-V5 were stained with Texas Red-labeled anti-V5 and FITC-labeled antibodies specific for markers of peroxisome, endoplasmic reticulum (ER), or Golgi and were visualized by confocal microscopy.

for A (TFAM) promoter.<sup>9</sup> TFAM acts as a link between the nucleus and the mitochondria by directly regulating mitochondrial DNA (mtDNA) replication and transcription. Transcription of PGC-1 $\alpha$  has been reported to be regulated by a variety of stimuli including hypoxia<sup>18</sup> and in a number of models of insulin deficiency.<sup>19</sup> In addition, post-translational modifications of the PGC-1 $\alpha$  protein have been shown to alter its stability and specificity toward binding partners. Protein degradation is one mechanism by which mitochondrial biogenesis is controlled, with several reports demonstrating that the proteasome is a key controller of PGC-1 $\alpha$  protein.<sup>20–22</sup>

Under pathologic conditions such as oxidative stress, an increase in mitochondrial biogenesis may occur as a compensatory mechanism in response to mitochondrial dysfunction and damage.<sup>23</sup> Oxidative stress is a key mediator of progressive T1F and ESRD,<sup>24–27</sup> and recovery of renal proximal tubular cells from oxidative stress has been shown to be accompanied by an increase in PGC-1 $\alpha$  protein.<sup>28,29</sup> This suggests that PGC-1 $\alpha$  is a potential target in regulating cellular bioenergetics in the kidney after injury.

Here we report that IHG-1 is a mitochondrial associated protein and that loss of endogenous IHG-1 results in a decrease in mitochondrial biogenesis. This is accompanied by a decrease in PGC-1 $\alpha$  protein, decreased expression of NRF-1 and TFAM, and reduced activation of a TFAM-sensitive promoter reporter construct. Conversely, overexpression of IHG-1 resulted in increased mitochondrial biogenesis through stabilization of PGC-1 $\alpha$  protein. Increased PGC-1 $\alpha$  protein was observed in the unilateral ureteral obstruction (UUO) model of renal fibrosis at both 3 and 10 days after obstruction. These data suggest that stabilization of PGC-1 $\alpha$  protein occurs in renal fibrosis concomitant with an increase in IHG-1 expression.

## RESULTS

### IHG-1 Is a Mitochondrial Associated Protein

To examine the subcellular localization of IHG-1, we generated stable cell lines expressing V5-tagged IHG-1 in both HeLa cells and in the renal proximal tubule cell line HK2, by lentiviral transduction. Overexpression of IHG-1 was confirmed by

real-time reverse transcription (RT)-PCR analysis (Figure 1, A and B) and immunoblotting (Figure 1C). Confocal analysis of immunofluorescent staining demonstrates that IHG-1 colocalizes with the mitochondrial marker manganese superoxide dismutase (MnSOD) in both cell lines (Figure 1D). Subcellular fractionation and immunoblotting further confirmed the localization of overexpressed IHG-1 to the mitochondria (Figure 1E). Importantly, we have also confirmed the mitochondrial localization of endogenous IHG-1 in both HeLa and HK2 cells (Figure 1F). Overexpressed IHG-1 did not colocalize to other cellular membrane compartments. Confocal analysis indicated that IHG-1 does not colocalize with markers for the peroxisome, endoplasmic reticulum, or Golgi apparatus (Figure 1G), confirming that IHG-1 is a mitochondrial associated protein.

### PGC-1 $\alpha$ Protein Is Increased in Experimental Renal Fibrosis

Subcellular fractionation and Western blotting of rat kidney tissue confirmed that IHG-1 colocalizes with the mitochondrial marker MnSOD (Figure 2A). Glyceraldehyde-3-phosphate dehydrogenase (GAPDH) was not detected. We have previously shown that IHG-1 expression is significantly increased in UUO at both 3 and 10 days.<sup>4</sup> Three days after ligation of the ureter, interstitial inflammation and tubular dilation were evident in the ligated kidney.<sup>4</sup> Ten days after ligation, TIF was evident in the ligated kidney, and considerable collagen deposition was detected by Gomorri trichrome staining (Figure 2B). Increased  $\alpha$ -smooth muscle actin was seen at both days 3 and 10 after UUO (Figure 2C). PGC-1 $\alpha$  mRNA was found to be reduced in ligated kidneys compared with nonligated kidneys at both timepoints (Figure 2D). However, despite a reduction in PGC-1 $\alpha$  mRNA, increased PGC-1 $\alpha$  protein was detected in these samples (Figure 2E). These data indicate that increased IHG-1 expression is associated with increased PGC-1 $\alpha$  protein in an *in vivo* model of TIF.

### Loss of Endogenous IHG-1 Expression Results in Decreased Mitochondrial Biogenesis

To investigate the possibility that IHG-1 is involved in mitochondrial biogenesis, we generated stable HeLa cell lines expressing tetracycline-inducible IHG-1-specific short hairpin RNA interference (shRNAi) or a scrambled shRNAi control (Scr). Knockdown of IHG-1 expression was confirmed by real-time RT-PCR (Figure 3A) and immunoblotting (Figure 3B). Mitochondrial mass was assessed by analyzing mtDNA. Reduction of IHG-1 expression resulted in a significant (1.4-fold) reduction in mtDNA (Figure 3C).

Mitochondrial mass was also measured in cells stably overexpressing IHG-1 by flow cytometric analysis of the fluorescence mitochondrial marker MitoTracker Red.<sup>30,31</sup> A significant increase in fluorescence (38%) was seen in IHG-1 overexpressing cells compared with controls, denoting an increase in mitochondrial mass (Figure 4A). A deletion mutant of IHG-1 lacking the mitochondrial targeting sequence ( $\Delta$ mts-IHG-1) has been found to no longer localize to the mitochon-

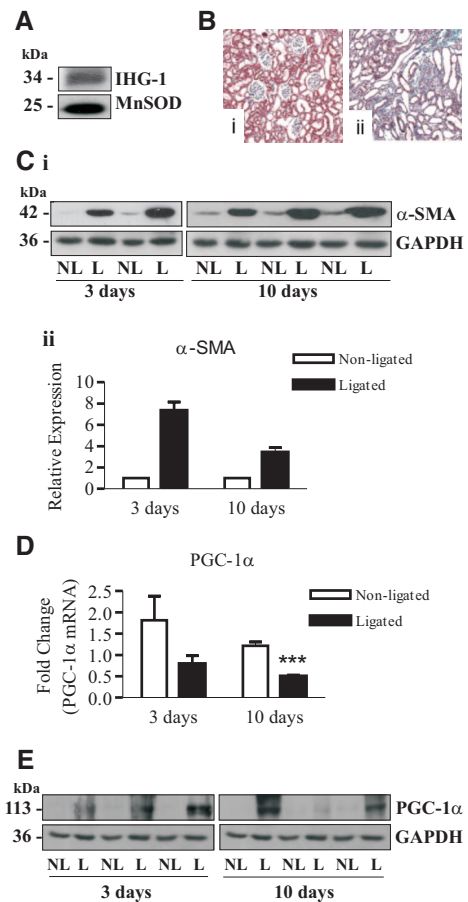


**Figure 2.** Peroxisome proliferator-activated receptor  $\gamma$  coactivator-1 $\alpha$  (PGC-1 $\alpha$ ) protein is increased in the unilateral ureteral obstruction (UUO) model of kidney fibrosis. (A) Mitochondrial protein cell extract was prepared from rat kidney tissue and was analyzed by immunoblotting with antibodies specific for endogenous Induced-by-High-Glucose 1 (IHG-1) and manganese superoxide dismutase (MnSOD). (B) Histologic detection of tubulointerstitial fibrosis (TIF) in UUO using Gomorri trichrome staining (magnification,  $\times 20$ ) of a 10-day nonligated (panel i) and ligated (panel ii) rat kidney illustrating increased collagen in the tubulointerstitium. (C) Protein extracts were prepared from rat nonligated (NL) and ligated (L) kidneys 3 and 10 days after UUO. These samples were analyzed by immunoblotting with antibodies specific for  $\alpha$ -smooth muscle actin ( $\alpha$ -SMA). Glyceraldehyde-3-phosphate dehydrogenase (GAPDH) demonstrates equal protein loading. (D) RNA was isolated from rat nonligated (NL) and ligated (L) kidneys 3 and 10 days after UUO. PGC-1 $\alpha$  mRNA expression was quantified by real-time RT-PCR ( $n = 6$ ). (E) Protein extracts from C were analyzed by immunoblotting with antibodies specific for PGC-1 $\alpha$ . GAPDH demonstrates equal protein loading. \*\*\*,  $P < 0.001$  (mean  $\pm$  SEM).

dria (J.B. Corcoran, S. McCarthy, F.B. Hickey, B. Griffin, U. Bhreathnach, F. Furlong, F. Martin, C. Godson, and M. Murphy, manuscript in preparation). Overexpression of  $\Delta$ mts-IHG-1 did not effect mitochondrial mass, indicating that mitochondrial localization of IHG-1 is required (Figure 4A). Increased mitochondrial mass in response to overexpression of

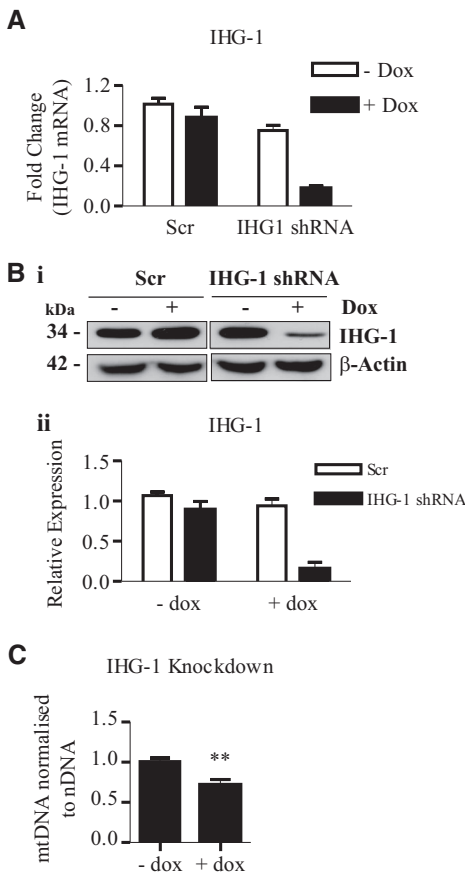


**Figure 3.** Loss of endogenous Induced-by-High-Glucose 1 (IHG-1) expression results in decreased mitochondrial biogenesis. (A) IHG-1 mRNA was quantified by real-time RT-PCR in HeLa cells stably expressing tetracycline-inducible short hairpin RNA interference (shRNAi) constructs specific for IHG-1 or with a scrambled construct (Scr) cultured in the presence or absence of doxycycline (Dox) for 96 hours. (B) Whole-cell lysates from cells in A were analyzed by immunoblotting with antibodies specific for IHG-1 (panel i).  $\beta$ -Actin demonstrates equal protein loading. Densitometric analysis of Western blots is shown (panel ii). (C) Mitochondrial DNA (mtDNA) was analyzed by real-time PCR. The results were normalized to nuclear DNA (nDNA) and are expressed relative to control cells (- dox). \*\*,  $P < 0.01$  (mean  $\pm$  SEM;  $n = 3$  throughout).

IHG-1 was associated with a 1.4-fold increase in mtDNA (Figure 4B). We further confirmed increased mitochondrial mass in IHG-1-overexpressing cells by fluorescence imaging after incubation with MitoTracker Red (Figure 4C). In combination, these data demonstrate that a loss of endogenous IHG-1 expression leads to decreased mitochondrial biogenesis, whereas overexpressing IHG-1 leads to an increase in mitochondrial mass. In addition, IHG-1 must be localized to the mitochondria to mediate its effects on mitochondrial biogenesis.

### IHG-1 Regulates the Expression of Mitochondrial Proteins

Altered mitochondrial biogenesis has been shown to be ac-

companied by differential expression of mitochondrial proteins including cytochrome  $c^{32}$  and MnSOD.<sup>33</sup> Decreased expression of both MnSOD and cytochrome  $c$  mRNA (Figure 5A) and protein (Figure 5B) were detected in cells in which IHG-1 expression was knocked down. Conversely, an increase in the expression of both MnSOD and cytochrome  $c$  mRNA (Figure 5C) and protein (Figure 5D) was observed after overexpression of IHG-1. These data indicate that altering the expression of IHG-1 results in differential expression of nuclear genes encoding mitochondrial proteins.

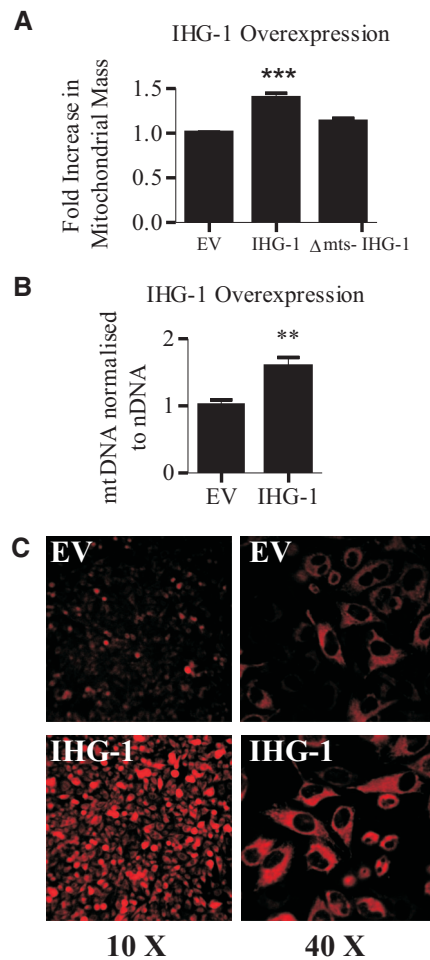


**Figure 4.** Overexpression of Induced-by-High-Glucose 1 (IHG-1) but not  $\Delta$ mts-IHG-1 results in increased mitochondrial biogenesis. (A) Mitochondrial mass was assessed in HeLa cells stably overexpressing either IHG-1,  $\Delta$ mts-IHG-1, or an empty vector control (EV) by flow cytometry after incubation with MitoTracker Red. Fold increase in mitochondrial mass was calculated from mean fluorescence intensities. (B) Mitochondrial DNA (mtDNA) was analyzed by real-time PCR. The results were normalized to nuclear DNA (nDNA) and are expressed relative to control cells (EV). (C) Cells overexpressing IHG-1 and control cells (EV) were visualized by fluorescence microscopy after incubation with MitoTracker Red. \*\*,  $P < 0.01$ ; \*\*\*,  $P < 0.001$  (mean  $\pm$  SEM;  $n = 3$  throughout).

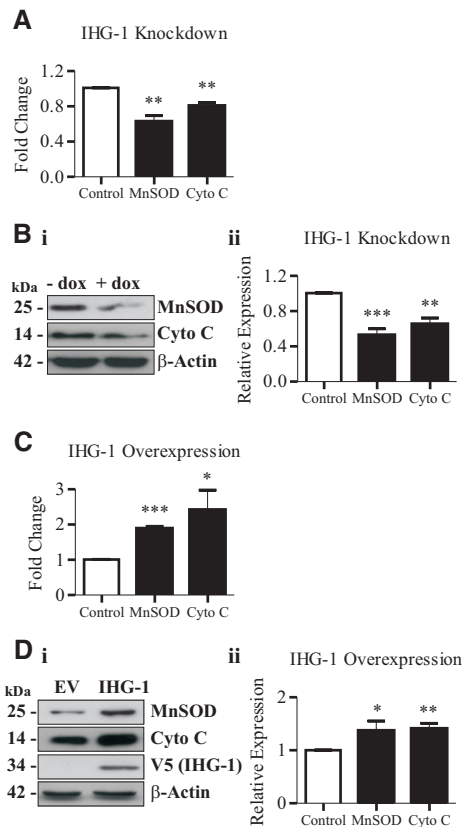


**Figure 5.** Expression of Induced-by-High-Glucose 1 (IHG-1) regulates expression of mitochondrial proteins manganese superoxide dismutase (MnSOD) and cytochrome (Cyto) c. (A) MnSOD and cytochrome c mRNA were quantified by real-time RT-PCR in HeLa cells expressing tetracycline-inducible IHG-1-specific shRNAi (+ dox) and control cells (– dox). (B) Whole-cell lysates from cells in A were analyzed by immunoblotting with antibodies specific for MnSOD or cytochrome c (panel i).  $\beta$ -Actin demonstrates equal protein loading. Densitometric analysis of Western blots is shown (panel ii). (C) MnSOD and cytochrome c (Cyto c) mRNA was quantified by real-time RT-PCR in HeLa cells overexpressing IHG-1 and control cells (EV). (D) Whole-cell lysates from cells in C were analyzed by immunoblotting with antibodies specific for MnSOD or cytochrome c (panel i). Overexpression of IHG-1 was confirmed by immunoblotting with anti-V5.  $\beta$ -Actin demonstrates equal protein loading. Densitometric analysis of Western blots is shown (panel ii). \*,  $P < 0.05$ ; \*\*,  $P < 0.01$ ; \*\*\*,  $P < 0.001$  (mean  $\pm$  SEM;  $n = 3$  throughout).

### Overexpression of IHG-1 Leads to Increased Stability of PGC-1 $\alpha$ Protein

Reduced mitochondrial biogenesis has been demonstrated to occur as a consequence of decreased PGC-1 $\alpha$  expression.<sup>32,11,29</sup> Loss of IHG-1 expression led to reductions in both PGC-1 $\alpha$  mRNA (Figure 6A) and protein (Figure 6B). Expression of the closely related homologue PGC-1 $\beta$ , which shares a similar role in mitochondrial biogenesis,<sup>34,13</sup> was unaltered (Figure 6A). In contrast, overexpressing IHG-1 did not alter the mRNA levels of either PGC-1 $\alpha$  or PGC-1 $\beta$  (Figure 6C). Interestingly, overexpression of IHG-1 was found to result in increased PGC-1 $\alpha$

protein (Figure 6D), suggesting that IHG-1 was modulating PGC-1 $\alpha$  protein stability. Consistent with this, we report that in cycloheximide-treated cells, PGC-1 $\alpha$  stability was significantly increased after IHG-1 overexpression (Figure 6E).

We further investigated the link between IHG-1 and PGC-1 $\alpha$  by overexpressing PGC-1 $\alpha$  in HeLa cells. Increased PGC-1 $\alpha$  expression was confirmed by both real-time RT-PCR (Figure 7A) and immunoblotting (Figure 7B). As reported,<sup>11,29,32</sup> increased mitochondrial mass was detected after overexpression of PGC-1 $\alpha$ , as measured by MitoTracker uptake (Figure 7C). We also detected increased IHG-1 mRNA in these cells by real-time RT-PCR (Figure 7D), confirming the upregulation of IHG-1 during mitochondrial biogenesis.

### IHG-1 Controls Expression of Key Transcription Factors Required for Mitochondrial Biogenesis

We found that the loss of IHG-1 expression led to reduced expression of NRF-1, a transcription factor activated by PGC-1 $\alpha$  (Figure 8A). NRF-1 has been shown to activate the transcription of a large number of nuclear encoded mitochondrial genes including TFAM,<sup>17</sup> a key regulator of mtDNA replication and transcription.<sup>35,36</sup> Reduced IHG-1 expression also resulted in decreased TFAM expression (Figure 8A). Decreased mRNA levels of two mitochondrially-encoded genes, cytochrome b (cyto b) and ATP synthase subunit 6 (Atp6), were also detected in response to the loss of IHG-1 expression (Figure 8B). Knockdown of endogenous IHG-1 expression also led to a reduction in basal activity from a transfected TFAM-sensitive promoter reporter construct.<sup>10</sup> In addition, overexpression of PGC-1 $\alpha$  in these cells did not significantly increase TFAM promoter activity (Figure 8C). Conversely, overexpression of IHG-1 led to an increase in expression of both NRF-1 and TFAM (Figure 8D). A consequent increase in expression of the mitochondrial encoded Atp6 and cytochrome b genes was also detected (Figure 8E). These data indicate that IHG-1 controls a program of mitochondrial biogenesis involving PGC-1 $\alpha$  and also downstream transcription factors and both nuclear and mitochondrial encoded genes.

### IHG-1 Increases PGC-1 $\alpha$ Protein in Tubular Epithelial Cells

Overexpression of IHG-1 in the renal proximal tubule cell line HK2 did not alter expression of PGC-1 $\alpha$  mRNA (Figure 9A). However, increased PGC-1 $\alpha$  protein was detected in these cells (Figure 9B). Overexpression of IHG-1 also led to a statistically significant increase in the expression of both TFAM and cytochrome c mRNA (Figure 9C). These data demonstrate that increased IHG-1 expression in renal tubule cells leads to increased mitochondrial biogenesis.

Expression levels of PGC-1 $\alpha$ -regulated transcripts were investigated in human DN using the gene expression database Nephromine (<http://www.nephromine.org/>). Previously published mRNA levels from human DN and control biopsies<sup>37</sup> were analyzed using OncoPrint<sup>TM</sup> (Compendia Bioscience, Ann Arbor, MI). IHG-1, cytochrome c, and MnSOD mRNA

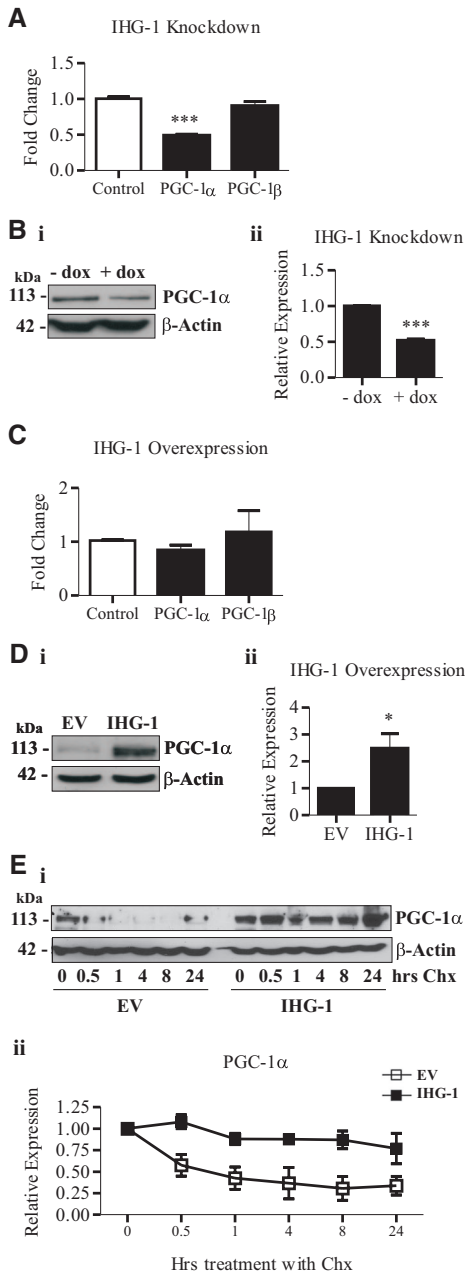


**Figure 6.** Induced-by-High-Glucose 1 (IHG-1) overexpression results in increased stability of peroxisome proliferator-activated receptor  $\gamma$  coactivator-1 $\alpha$  (PGC-1 $\alpha$ ) protein. (A) PGC-1 $\alpha$  and peroxisome proliferator-activated receptor  $\gamma$  coactivator-1 $\beta$  (PGC-1 $\beta$ ) mRNA was quantified by real-time RT-PCR in HeLa cells expressing tetracycline-inducible IHG-1-specific shRNAi (+ dox) and control cells (– dox). (B) Whole-cell lysates from cells in A were analyzed by immunoblotting with antibodies specific for PGC-1 $\alpha$  (panel i).  $\beta$ -Actin demonstrates equal protein loading. Densitometric analysis of Western blots is shown (panel ii). (C) PGC-1 $\alpha$  and PGC-1 $\beta$  mRNA was quantified by real-time RT-PCR in HeLa cells stably overexpressing IHG-1 and empty vector cells (control). (D) Whole-cell lysates from cells in C were analyzed by immunoblotting with antibodies specific for PGC-1 $\alpha$  (panel i).  $\beta$ -Actin demonstrates equal protein loading. Densitometric

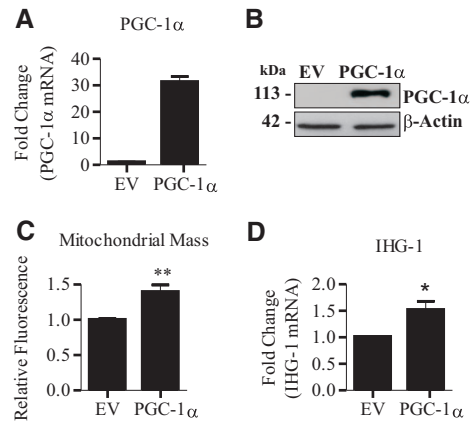


**Figure 7.** Overexpression of peroxisome proliferator-activated receptor  $\gamma$  coactivator-1 $\alpha$  (PGC-1 $\alpha$ ) leads to increased Induced-by-High-Glucose 1 (IHG-1) expression. (A) PGC-1 $\alpha$  mRNA was quantified by real-time RT-PCR in HeLa cells stably overexpressing PGC-1 $\alpha$  and control cells (EV). (B) Whole-cell lysates from cells in A were analyzed by immunoblotting with antibodies specific for PGC-1 $\alpha$ .  $\beta$ -Actin demonstrates equal protein loading. (C) Mitochondrial mass was assessed in HeLa cells stably overexpressing PGC-1 $\alpha$  or an empty vector control (EV) by flow cytometry after incubation with MitoTracker Red. Fold increase in mitochondrial mass was calculated from mean fluorescence intensities. (D) IHG-1 mRNA was quantified by real-time RT-PCR in cells from A. \*,  $P < 0.05$ ; \*\*,  $P < 0.01$  (mean  $\pm$  SEM;  $n = 3$  throughout).

levels were significantly increased in human DN ( $P = 2.1 \times 10^{-5}$ , 0.036, and 0.004 respectively). NRF-1 and TFAM mRNA levels were unchanged (Table 1).

## DISCUSSION

Mitochondria play a central role in energy homeostasis, metabolism, signaling, and apoptosis. As such, mitochondrial function and the rates of mitochondrial biogenesis and degradation are critical to the health and survival of cells. These processes are finely tuned to meet cell-specific demands and rely upon the integrated expression of both nuclear and mitochondrial genes.<sup>7</sup> The transcriptional coactivator PGC-1 $\alpha$  is a key mediator of this integrated program of mitochondrial biogenesis. In this study, we demonstrate that a loss of endogenous IHG-1 expression results in decreased mitochondrial biogenesis and reduced PGC-1 $\alpha$  expression. Conversely, overexpression of IHG-1 led to increased mitochondrial biogenesis through the stabilization of PGC-1 $\alpha$  protein. Mitochondrial localization of IHG-1 is required for its effect on mitochondrial

analysis of Western blots is shown (panel ii). (E) HeLa cells stably overexpressing IHG-1 and control cells (EV) were treated with 20  $\mu$ g/ml cycloheximide (Chx) for the indicated times. Whole-cell lysates were analyzed by immunoblotting with antibodies specific for PGC-1 $\alpha$  (panel i).  $\beta$ -Actin demonstrates equal protein loading. Densitometric analysis of Western blots is shown (panel ii). \*,  $P < 0.05$ ; \*\*\*,  $P < 0.001$  (mean  $\pm$  SEM;  $n = 3$  throughout).

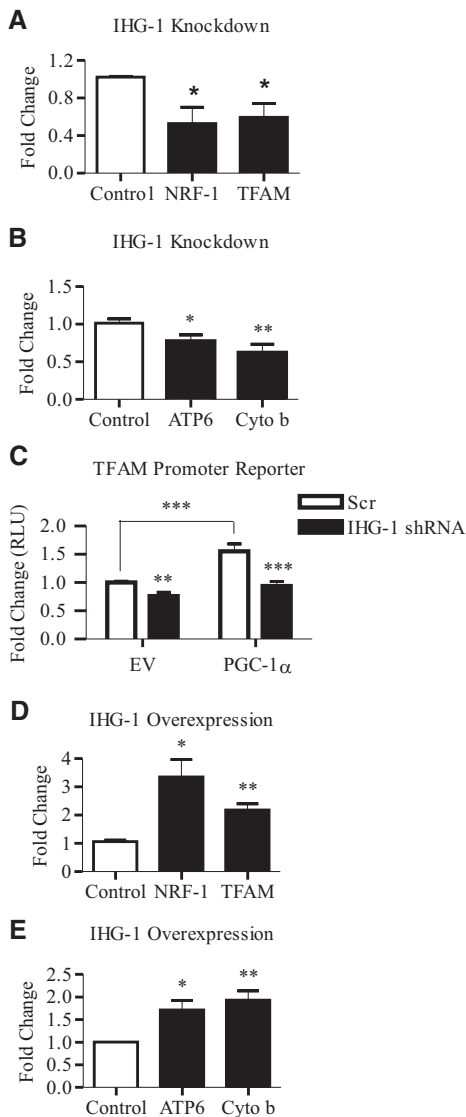


**Figure 8.** Expression levels of Induced-by-High-Glucose 1 (IHG-1) correlate with levels of key mediators of mitochondrial biogenesis. (A) nuclear respiratory factor 1 (NRF-1) and mitochondrial transcription factor A (TFAM) mRNA was quantified by real-time RT-PCR in HeLa cells expressing tetracycline-inducible IHG-1-specific short hairpin RNA interference (shRNAi) and control cells. (B) ATP synthase subunit 6 (ATP6) and cytochrome (Cyto) b mRNA was quantified by real-time RT-PCR in cells from A. (C) HeLa cells expressing tetracycline-inducible IHG-1-specific shRNAi or control Scr cells, cultured in the presence of doxycycline, were cotransfected with the TFAM promoter reporter and phRL-CMV, an internal control reporter driving expression of *Renilla* luciferase, with or without pcDNA4-Myc-PGC-1 $\alpha$  expression plasmid as indicated. Firefly luciferase activity normalized to *Renilla* luciferase activity was determined. (D) NRF-1 and TFAM mRNA was quantified by real-time RT-PCR in HeLa cells stably overexpressing IHG-1 and empty vector cells (control). (E) ATP6 and cytochrome b mRNA was quantified by real-time RT-PCR in cells from C. \*,  $P < 0.05$ ; \*\*,  $P < 0.01$ ; \*\*\*,  $P < 0.001$  (mean  $\pm$  SEM;  $n = 3$  throughout).

biogenesis, because overexpression of a deletion mutant of IHG-1 lacking the mitochondrial targeting sequence does not significantly alter mitochondrial mass.

Mitochondrial biogenesis is regulated by several intracellular and extracellular factors including oxidative stress,<sup>29</sup> calcium ion concentration,<sup>38</sup> nitric oxide,<sup>39</sup> and insulin.<sup>40</sup> All of these factors have been implicated in the pathogenesis or treatment of various conditions resulting in renal fibrosis.<sup>41–44</sup> Significantly, IHG-1 expression has been shown to be increased in both DN and an experimental model of renal fibrosis (UUO) in which TIF is well modeled.<sup>4,45</sup> Oxidative stress is a key early event in both of these conditions.<sup>25–27</sup> In DN, the source of increased ROS is believed to be mitochondrial,<sup>25,26</sup> and a recent study demonstrated that a mitochondrion-targeted antioxidant (MitoQ) improved tubular and glomerular function in the *Ins2*<sup>+/-Akita</sup> mouse model of type 1 diabetes.<sup>46</sup> In the UUO model, antioxidant peptides targeted to the inner mitochondrial membrane have been shown to protect against renal damage.<sup>27</sup> In addition, PGC-1 $\alpha$  protein has been shown to be increased in renal tubular epithelial cells after short-term oxidative stress, leading to increased mitochondrial biogenesis and cell recovery. This may be an initial protective response, because PGC-1 $\alpha$  levels return to basal after 6 days.<sup>29</sup> IHG-1 may play an important role in the sensing of cellular damage leading to increased PGC-1 $\alpha$  protein levels and thus increasing mitochondrial biogenesis. This is supported by the observed increase in PGC-1 $\alpha$  protein in the ligated kidneys of UUO rats

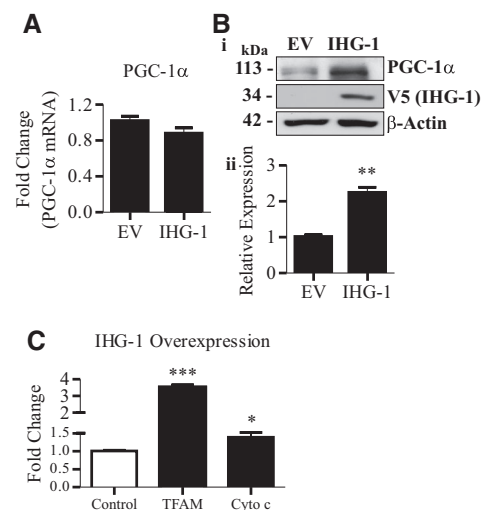


**Figure 9.** Peroxisome proliferator-activated receptor  $\gamma$  coactivator-1 $\alpha$  (PGC-1 $\alpha$ ) protein is increased in renal proximal tubular epithelial cells. (A) PGC-1 $\alpha$  mRNA was quantified by real-time RT-PCR in HK2 cells stably overexpressing Induced-by-High-Glucose 1 (IHG-1) and control cells (EV). (B) PGC-1 $\alpha$  protein expression was determined in cells from A by immunoblotting (panel i).  $\beta$ -Actin demonstrates equal protein loading. Densitometric analysis of Western blots is shown (panel ii). (C) Mitochondrial transcription factor A (TFAM) and cytochrome (Cyto) c mRNA was quantified by real-time RT-PCR in cells from A. \*,  $P < 0.05$ ; \*\*,  $P < 0.01$ ; \*\*\*,  $P < 0.001$  (mean  $\pm$  SEM;  $n = 3$  throughout).

**Table 1.** Expression of peroxisome proliferator-activated receptor  $\gamma$  coactivator-1 $\alpha$  (PGC-1 $\alpha$ )-regulated genes in human diabetic nephropathy (DN)

	P
Increased mRNA in DN	
IHG-1	$2.1 \times 10^{-5}$
Cytochrome	0.036
MnSOD	0.004
Unaltered mRNA in DN	
NRF-1	0.224
TFAM	0.314
Decreased mRNA in DN	
PGC-1 $\alpha$	0.003

Previously published mRNA levels from human DN and control biopsies were analyzed using Oncomime (Compendia Bioscience, Ann Arbor, MI). IHG-1, Induced-by-High-Glucose 1; NRF-1, nuclear respiratory factor 1; TFAM, mitochondrial transcription factor A; PGC-1 $\alpha$ , peroxisome proliferator-activated receptor  $\gamma$  coactivator 1 $\alpha$ ; MnSOD, manganese superoxide dismutase.

despite reductions in PGC-1 $\alpha$  mRNA, suggesting that increased stabilization of PGC-1 $\alpha$  protein is occurring in this model in association with increased expression of IHG-1.<sup>4</sup> Furthermore, analysis of gene expression in human DN using the gene expression database Nephromine, indicated that although expression of cytochrome c and MnSOD were increased, PGC-1 $\alpha$  mRNA levels were not. These data mirror our findings *in vitro*, where increased mitochondrial biogenesis is due to increased PGC-1 $\alpha$  protein, not mRNA.

Transcription factors activated by PGC-1 $\alpha$  include NRF-1, NRF-2, peroxisome proliferator-activated receptor  $\alpha$ , estrogen-related receptor  $\alpha$  (ERR $\alpha$ ), Sp1, and others. Specific NRF-1 binding sites have been identified in the promoters of several nuclear genes required for mitochondrial respiratory function, including cytochrome c.<sup>47,48</sup> TFAM is a master regulator of mtDNA replication and transcription and, as a nuclear encoded gene, acts as a link between the nucleus and mitochondria during mitochondrial biogenesis.<sup>8</sup> NRF-1 has been shown to bind to and activate the TFAM promoter.<sup>35,36</sup> Along with decreased expression of cytochrome c and MnSOD, we have also demonstrated decreased NRF-1 and TFAM expression in response to loss of IHG-1. These data indicate that IHG-1 controls a program of mitochondrial biogenesis involving PGC-1 $\alpha$  and also downstream transcription factors and both nuclear and mitochondrial encoded genes. In addition, overexpression of IHG-1 expression resulted in increased mitochondrial biogenesis along with increased expression of key transcription factors (NRF-1 and TFAM) and both nuclear and mitochondrial encoded genes (MnSOD, cytochrome c, cytochrome b, and ATP6), all targets of PGC-1 $\alpha$ . These data further suggest that IHG-1 regulates mitochondrial biogenesis and function via its modulation of PGC-1 $\alpha$  stability.

Mitochondrial biogenesis is a highly controlled process. To achieve this, both the expression and activity of PGC-1 $\alpha$  are tightly regulated. Whereas mechanisms by which transcription of PGC-1 $\alpha$  is activated have been well studied,<sup>14,39,49,50</sup> the regulation of the half-life of the PGC-1 $\alpha$  protein is poorly under-

stood. Although increased PGC-1 $\alpha$  expression has been associated with recovery from cell stress, evidence also suggests that sustained activation of PGC-1 $\alpha$  is not desirable and may even be pathogenic. Lehman *et al.*<sup>11</sup> have demonstrated that overexpression of PGC-1 in cardiac myocytes increased cellular mitochondrial number and stimulated coupled respiration. However, this ultimately resulted in a loss of sarcomeric structure and a dilated cardiomyopathy.

Several different mechanisms have been shown to alter the stability of PGC-1 $\alpha$  and also its specificity toward its binding partners. For example, PGC-1 $\alpha$  has been shown to be a target for ubiquitination and proteasomal degradation.<sup>20,51</sup> Other post-translational modifications include methylation,<sup>52</sup> and O-linked  $\beta$ -N-acetylglucosamination.<sup>53</sup> PGC-1 $\alpha$  activity can also be regulated by acetylation.<sup>54,55</sup> In addition, PGC-1 $\alpha$  can be degraded by calpains in response to Ca<sup>2+</sup> and oxidant injury.<sup>51</sup> Further investigation is required to determine the post-transcriptional/post-translational mechanism by which IHG-1 increases the stability of PGC-1 $\alpha$ . Of significant interest is the fact that only IHG-1 localized to the mitochondria increases mitochondrial biogenesis. Because IHG-1 is localized to the mitochondria, it is most likely that a complex signaling cascade is involved in altering the stability of PGC-1 $\alpha$ . At least four putative E3 ubiquitin ligases have been identified that are localized to the mitochondria.<sup>56</sup> PGC-1 $\alpha$  was previously believed to be predominantly located in the cytosol in resting cells and to translocate to the nucleus after external stimuli such as exercise that induce mitochondrial biogenesis.<sup>57</sup> However, Aquilano *et al.*<sup>58</sup> have recently demonstrated the presence of PGC-1 $\alpha$  inside mitochondria. In addition, a number of signaling pathways have been identified between the mitochondria and the nucleus. In one such example, Arnold *et al.*<sup>59</sup> have shown that peptides generated by the degradation of mitochondrial proteins provide a link between mitochondria and nuclear gene expression. Mass spectrometry analysis of binding partners of IHG-1 carried out by our group suggests that IHG-1 does not directly bind PGC-1 $\alpha$  (U. Bhreathnach, B. Griffin, F.B. Hickey, J.B. Corcoran, F. Martin, C. Godson, and M. Murphy, manuscript in preparation). In summary, this study identifies a critical role for IHG-1 in the stabilization of PGC-1 $\alpha$ , the master regulator of mitochondrial biogenesis.

## CONCISE METHODS

### Cell Culture

All of the cell lines were obtained from ATCC (Middlesex, UK). HEK293T and HeLa cells were cultured in DMEM and MEM, respectively, containing 10% FBS, 2 mM L-glutamine, 100 units/ml penicillin, and 1 mg/ml streptomycin (all from Invitrogen, Paisley, UK). HK2 cells were cultured in low glucose DMEM-F12 (1 g/L glucose) (Invitrogen), 2 mM glutamax (Invitrogen), 10 mM HEPES (Sigma-Aldrich, Dublin, Ireland), 10 ng/ml EGF (Sigma-Aldrich), 36 ng/ml hydrocortisone (Sigma-Aldrich), ITS (10  $\mu$ g/ml insulin, 5.5  $\mu$ g/ml transferrin, and 5 ng/ml sodium selenite) (Sigma-Aldrich), 3 pg/ml triiodothyronine (Sigma-

**Table 2.** Primer sequences used

Gene	Primer Sequence
MnSOD	F: tctggacaacacctagccct R: gcaactcccccttggggttc
Cytochrome c	F: tgaagtgttccacgtgccac R: cagctctgtgcttgcctccc
TFAM	F: actgcgtcccccttcag R: acagatgaaaaccacctcgtaa
NRF-1	F: acggaaacggcctcatgtat R: tgccctgctccggatagatgg
ATP synthase subunit 6	F: aaccgctaacattactgcagcc R: gcgaaggtaatccacgta
Cytochrome b	F: cgcatgatgaaacttcggct R: taaacctctagtccgtccg
MT-ND3	F: ttttaataatcaacacctctagcct R: agccgttgagttgtgtagtca
UCP2	F: tgtgggtgtaagtgcggatcc R: tccttttgttgggccagtt

F, forward; R, reverse; TFAM, mitochondrial transcription factor A; NRF-1, nuclear respiratory factor 1; MT-ND3, NADH dehydrogenase subunit 3; UCP2, mitochondrial uncoupling protein 2; MnSOD, manganese superoxide dismutase.

Aldrich), 25 ng/ml prostaglandin E1 (Sigma-Aldrich), 100 units/ml penicillin, and 1 mg/ml streptomycin (Invitrogen). Where indicated, the cells were treated with 20  $\mu$ g/ml cycloheximide (Merck Biosciences, Nottingham, UK).

### Stable Transduction of Cells

$\Delta$ mts-IHG-1 (deletion of amino acids 9 to 22) was generated using the QuikChange site-directed mutagenesis kit (Stratagene, Agilent Technologies, Cork, Ireland). Recombinant lentivirus was produced by transfection of HEK293T cells with pCMV $\Delta$ R8.9, pMD.2G, pLenti4/TO/IHG-1-V5, pLenti4/TO/ $\Delta$ mts-IHG-1-V5, pTRIPZ/Scr, pTRIPZ/IHG-1 shRNAi, pLenti6/PGC-1 $\alpha$  (Thermo Fisher Scientific, Surrey, UK), or empty vector controls using calcium phosphate transfection (Invitrogen). Stable cell lines were selected with appropriate antibiotic. Expression of tetracycline-inducible IHG-1 or Scr shRNAi was induced by culturing cells in the presence of 1  $\mu$ g/ml doxycycline (Sigma-Aldrich). For all of the experiments involving IHG-1 knock-down cells, Scr cells cultured in the presence and absence of doxycycline were also analyzed. No significant effects of doxycycline were observed.

### RNA Isolation and RT-PCR

Total RNA was extracted using TRIzol reagent (Invitrogen). 1  $\mu$ g of total RNA was reverse-transcribed using random primers and SuperScript II (Invitrogen). RT-PCR was performed on an Applied Biosystems 7900HT fast real-time PCR system using TaqMan gene-specific assays (Applied Biosystems, Warrington, UK) or gene-specific primers (MWG Biotech, Ebersberg, Germany) and SybrGreen (Table 2). The results were normalized to 18S rRNA expression. All PCRs were carried out as follows: 50°C for 2 minutes, 95°C for 10 minutes, 40 cycles of 95°C for 15 seconds, and 60°C for 1 minute.

### SDS-PAGE and Immunoblotting

Whole-cell extracts were prepared in radioimmune precipitation assay (RIPA) buffer (150 mM NaCl, 50 mM Tris-HCl, pH 7.4, 1 mM

EGTA, 1% Nonidet P-40, protease inhibitor mixture [Sigma-Aldrich], and phosphatase inhibitor cocktail [Roche, Burgess Hill, UK]). Protein content was quantified and normalized by using the Bradford method (Bio-Rad, Hemel Hempstead, UK). The proteins were separated by electrophoresis on SDS/PAGE gels. The antibodies used were: V5 (Invitrogen), MnSOD (Stressgen), GAPDH (Cell Signaling, Hertfordshire, UK), cytochrome c (Abcam, Cambridge, UK), PGC-1 $\alpha$  mouse mAb (4C1.3) (Merck), and  $\beta$ -actin (Sigma-Aldrich). The IHG-1 antibody to purified recombinant protein was generated by Open Biosystems (Huntsville, AL). Densitometric analysis was performed using Scion Image (Scion Corp., Frederick, MD).

### Immunofluorescence

The cells were fixed with 4% paraformaldehyde and permeabilized in 0.1% Triton X-100. The cells were blocked with 5% normal goat serum and incubated overnight at 4°C with primary antibodies. After washing, the cells were incubated with secondary antibodies conjugated to the indicated fluorophores for 1 hour at room temperature. The slides were then washed and mounted with ProLong Gold mounting medium (Invitrogen) containing 4',6'-diamino-2-phenylindole (DAPI) and anti-fade reagent. Confocal fluorescence images were obtained by a Zeiss LSM 510meta confocal scan head mounted on a Zeiss Axiovert 200M microscope using a 63 $\times$  oil immersion objective. The primary antibodies were: V5 (Invitrogen) and MnSOD (Stressgen, Ann Arbor, MI). The secondary antibodies were: Texas Red goat anti-mouse IgG and Alexa Fluor 488 goat anti-rabbit IgG (Invitrogen).

### Subcellular Fractionation

Mitochondria were purified using the Qproteome mitochondria isolation kit (Qiagen) as per the manufacturer's instructions. GAPDH and MnSOD were used as subcellular markers for the cytosol and mitochondria, respectively.

### Animals and Unilateral Ureteric Obstruction Surgery

UUO was carried out in male Wistar rats as described previously.<sup>4</sup> The experiments were carried out under a Department of Health and Children license (B100/3611). All of the animal usage was in accordance with the National Institutes of Health Guide for Care and Use of Laboratory Animals.

### Analysis of Mitochondrial DNA

Total genomic DNA was isolated using a GenElute mammalian genomic DNA kit (Sigma-Aldrich) according to the manufacturer's instructions. NADH dehydrogenase subunit 3 was used as a mtDNA marker, and mitochondrial uncoupling protein 2 was used as a nuclear DNA marker. NADH dehydrogenase subunit 3 primers were designed from regions of mitochondrial DNA that are not found in nuclear encoded mitochondrial pseudogenes. RT-PCR was performed as above using gene-specific primers and SybrGreen (Table 2). The results were normalized to uncoupling protein 2 DNA.

### MitoTracker Analysis

The cells were incubated with 5  $\mu$ M MitoTracker Red FM dye (Invitrogen) for 15 minutes and were washed once before analysis. For flow cytometry, all of the samples were analyzed using a Cyan ADP cytometry.

eter (Dako, Stockport, UK). For fluorescence microscopy, the cells were cultured on 8-well  $\mu$ -slides (Ibidi, Munich, Germany). Images were acquired with an Andor EMCCD camera (Andor, Belfast, Ireland) mounted on a Nikon Eclipse Ti microscope equipped with a Yokogawa CSU-X1 scan head (Yokogawa, Tokyo, Japan) using a 10 $\times$  or 40 $\times$  objective. All of the microscope settings including laser power were exactly replicated for control and test cell lines.

### TFAM Transcriptional Activation Assay

The cells were transfected with a human TFAM promoter reporter construct,<sup>10</sup> phRL-CMV (*Renilla* luciferase control reporter), and pcDNA4-Myc-PGC-1 $\alpha$ <sup>60</sup> or empty vector control using FuGENE transfection reagent (Roche). The cells were harvested 48 hours post-transfection, and luciferase activity was determined using a dual-luciferase reporter assay system (Promega, Southampton, UK). Firefly luciferase was normalized to *Renilla* luciferase.

### Statistical Analyses

All of the experiments were carried out with a minimum of  $n = 3$ . Inter-group comparisons were made by  $t$  test or one-way ANOVA using GraphPad Prism, with  $P < 0.05$  considered statistically significant.

### ACKNOWLEDGMENTS

This work was funded by Science Foundation Ireland, the Health Research Board, and the Government of Ireland Programme for Research in Third Level Institutions. We thank Andrew Gaffney, Dr. Dimitri Scholz, Ann Cullen, Dr. Alfonso Blanco, and Catherine Moss for technical assistance with fluorescence microscopy, flow cytometry, and real-time PCR in this study. We are grateful to Dr. Jane Jackman (Ohio State University) for purified recombinant IHG-1 protein, Dr. Ruth Gimeno (BioTex Pzifer, Cambridge, MA) for IHG-1 antibody, Prof. Didier Trono (University of Geneva) for pCMV $\Delta$ R8.9 and pMD.2G constructs, Prof. Richard C. Scarpulla (Northwestern University Medical School, Chicago, IL) for TFAM (TFAM) promoter reporter construct, and Dr. Toren Finkel (National Heart Lung and Blood Institute, National Institutes of Health, Bethesda, MD) for providing pcDNA4-Myc-PGC-1 $\alpha$  construct.

### DISCLOSURES

None.

### REFERENCES

- Liu Y: Renal fibrosis: New insights into the pathogenesis and therapeutics. *Kidney Int* 69: 213–217, 2006
- Wang W, Koka V, Lan HY: Transforming growth factor-beta and Smad signalling in kidney diseases. *Nephrology* 10: 48–56, 2005
- Murphy M, Godson C, Cannon S, Kato S, Mackenzie HS, Martin F, Brady HR: Suppression subtractive hybridization identifies high glucose levels as a stimulus for expression of connective tissue growth factor and other genes in human mesangial cells. *J Biol Chem* 274: 5830–5834, 1999
- Murphy M, Docherty NG, Griffin B, Howlin J, McArdle E, McMahon R, Schmid H, Kretzler M, Drogue A, Mezzano S, Brady HR, Furlong F, Godson C, Martin F: IHG-1 amplifies TGF-beta1 signaling and is increased in renal fibrosis. *J Am Soc Nephrol* 19: 1672–1680, 2008
- Ziyadeh FN: Mediators of diabetic renal disease: The case for tgf-beta as the major mediator. *J Am Soc Nephrol* 15[Suppl 1]: S55–S57, 2004
- Krupa A, Jenkins R, Luo DD, Lewis A, Phillips A, Fraser D: Loss of MicroRNA-192 promotes fibrogenesis in diabetic nephropathy. *J Am Soc Nephrol* 21: 438–447, 2010
- Garesse R, Vallejo CG: Animal mitochondrial biogenesis and function: A regulatory cross-talk between two genomes. *Gene* 263: 1–16, 2001
- Kelly DP, Scarpulla RC: Transcriptional regulatory circuits controlling mitochondrial biogenesis and function. *Genes Dev* 18: 357–368, 2004
- Puigserver P, Wu Z, Park CW, Graves R, Wright M, Spiegelman BM: A cold-inducible coactivator of nuclear receptors linked to adaptive thermogenesis. *Cell* 92: 829–839, 1998
- Wu Z, Puigserver P, Andersson U, Zhang C, Adelmant G, Mootha V, Troy A, Cinti S, Lowell B, Scarpulla RC, Spiegelman BM: Mechanisms controlling mitochondrial biogenesis and respiration through the thermogenic coactivator PGC-1. *Cell* 98: 115–124, 1999
- Lehman JJ, Barger PM, Kovacs A, Saffitz JE, Medeiros DM, Kelly DP: Peroxisome proliferator-activated receptor gamma coactivator-1 promotes cardiac mitochondrial biogenesis. *J Clin Invest* 106: 847–856, 2000
- Lin J, Wu H, Tarr PT, Zhang CY, Wu Z, Boss O, Michael LF, Puigserver P, Isotani E, Olson EN, Lowell BB, Bassel-Duby R, Spiegelman BM: Transcriptional co-activator PGC-1 alpha drives the formation of slow-twitch muscle fibres. *Nature* 418: 797–801, 2002
- St-Pierre J, Lin J, Krauss S, Tarr PT, Yang R, Newgard CB, Spiegelman BM: Bioenergetic analysis of peroxisome proliferator-activated receptor gamma coactivators 1 $\alpha$  and 1 $\beta$  (PGC-1 $\alpha$  and PGC-1 $\beta$ ) in muscle cells. *J Biol Chem* 278: 26597–26603, 2003
- Puigserver P, Spiegelman BM: Peroxisome proliferator-activated receptor-gamma coactivator 1 alpha (PGC-1 alpha): Transcriptional coactivator and metabolic regulator. *Endocr Rev* 24: 78–90, 2003
- Handschin C, Spiegelman BM: Peroxisome proliferator-activated receptor gamma coactivator 1 coactivators, energy homeostasis, and metabolism. *Endocr Rev* 27: 728–735, 2006
- Gleyzer N, Vercauteren K, Scarpulla RC: Control of mitochondrial transcription specificity factors (TFB1M and TFB2M) by nuclear respiratory factors (NRF-1 and NRF-2) and PGC-1 family coactivators. *Mol Cell Biol* 25: 1354–1366, 2005
- Scarpulla RC: Nuclear control of respiratory chain expression in mammalian cells. *J Bioenerg Biomembr* 29: 109–119, 1997
- Zhu L, Wang Q, Zhang L, Fang Z, Zhao F, Lv Z, Gu Z, Zhang J, Wang J, Zen K, Xiang Y, Wang D, Zhang CY: Hypoxia induces PGC-1 $\alpha$  expression and mitochondrial biogenesis in the myocardium of TOF patients. *Cell Res* 20: 676–687, 2010
- Yoon JC, Puigserver P, Chen G, Donovan J, Wu Z, Rhee J, Adelmant G, Stafford J, Kahn CR, Granner DK, Newgard CB, Spiegelman BM: Control of hepatic gluconeogenesis through the transcriptional coactivator PGC-1. *Nature* 413: 131–138, 2001
- Anderson RM, Barger JL, Edwards MG, Braun KH, O'Connor CE, Prolla TA, Weindrich R: Dynamic regulation of PGC-1 $\alpha$  localization and turnover implicates mitochondrial adaptation in calorie restriction and the stress response. *Aging Cell* 7: 101–111, 2008
- Olson BL, Hock MB, Ekholm-Reed S, Wohlschlegel JA, Dev KK, Kralli A, Reed SI: SCFCdc4 acts antagonistically to the PGC-1 $\alpha$  transcriptional coactivator by targeting it for ubiquitin-mediated proteolysis. *Genes Dev* 22: 252–264, 2008
- Sano M, Tokudome S, Shimizu N, Yoshikawa N, Ogawa C, Shirakawa K, Endo J, Katayama T, Yuasa S, Ieda M, Makino S, Hattori F, Tanaka H, Fukuda K: Intramolecular control of protein stability, subnuclear compartmentalization, and coactivator function of peroxisome proliferator-activated receptor  $\gamma$  coactivator 1 $\alpha$ . *J Biol Chem* 282: 25970–25980, 2007

23. Suliman HB, Carraway MS, Welty-Wolf KE, Whorton AR, Piantadosi CA: Lipopolysaccharide stimulates mitochondrial biogenesis via activation of nuclear respiratory factor-1. *J Biol Chem* 278: 41510–41518, 2003
24. Djamali A: Oxidative stress as a common pathway to chronic tubulointerstitial injury in kidney allografts. *Am J Physiol Renal Physiol* 293: F445–F455, 2007
25. Nishikawa T, Edelstein D, Du XL, Yamagishi S, Matsumura T, Kaneda Y, Yorek MA, Beebe D, Oates PJ, Hammes HP, Giardino I, Brownlee M: Normalizing mitochondrial superoxide production blocks three pathways of hyperglycaemic damage. *Nature* 404: 787–790, 2000
26. Prabhakar S, Starnes J, Shi S, Lonis B, Tran R: Diabetic nephropathy is associated with oxidative stress and decreased renal nitric oxide production. *J Am Soc Nephrol* 18: 2945–2952, 2007
27. Mizuguchi Y, Chen J, Seshan SV, Poppas DP, Szeto HH, Felsen D: A novel cell-permeable antioxidant peptide decreases renal tubular apoptosis and damage in unilateral ureteral obstruction. *Am J Physiol Renal Physiol* 295: F1545–F1553, 2008
28. Nowak G, Aleo MD, Morgan JA, Schnellmann RG: Recovery of cellular functions following oxidant injury. *Am J Physiol* 274: F509–F515, 1998
29. Rasbach KA, Schnellmann RG: Signaling of mitochondrial biogenesis following oxidant injury. *J Biol Chem* 282: 2355–2362, 2007
30. Yu Y, Niapour M, Zhang Y, Berger SA: Mitochondrial regulation by c-Myc and hypoxia-inducible factor-1 alpha controls sensitivity to econazole. *Mol Cancer Ther* 7: 483–491, 2008
31. Marques-Santos LF, Oliveira JG, Maia RC, Rumjanek VM: Mitotracker green is a P-glycoprotein substrate. *Biosci Rep* 23: 199–212, 2003
32. O'Hagan KA, Cocchiglia S, Zhdanov AV, Tambuwala MM, Cummins EP, Monfared M, Agbor TA, Garvey JF, Papkovsky DB, Taylor CT, Allan BB: PGC-1alpha is coupled to HIF-1alpha-dependent gene expression by increasing mitochondrial oxygen consumption in skeletal muscle cells. *Proc Natl Acad Sci U S A* 106: 2188–2193, 2009
33. Fujisawa K, Nishikawa T, Kukidome D, Imoto K, Yamashiro T, Motoshima H, Matsumura T, Araki E: TZDs reduce mitochondrial ROS production and enhance mitochondrial biogenesis. *Biochem Biophys Res Commun* 379: 43–48, 2009
34. Lin J, Puigserver P, Donovan J, Tarr P, Spiegelman BM: Peroxisome proliferator-activated receptor gamma coactivator 1 beta (PGC-1beta), a novel PGC-1-related transcription coactivator associated with host cell factor. *J Biol Chem* 277: 1645–1648, 2002
35. Clayton DA: Transcription and replication of animal mitochondrial DNAs. *Int Rev Cytol* 141: 217–232, 1992
36. Shadel GS, Clayton DA: Mitochondrial transcription initiation: Variation and conservation. *J Biol Chem* 268: 16083–16086, 1993
37. Schmid H, Boucherot A, Yasuda Y, Henger A, Brunner B, Eichinger F, Nitsche A, Kiss E, Bleich M, Grone HJ, Nelson PJ, Schlondorff D, Cohen CD, Kretzler M: Modular activation of nuclear factor-kappaB transcriptional programs in human diabetic nephropathy. *Diabetes* 55: 2993–3003, 2006
38. Wu H, Kanatous SB, Thurmond FA, Gallardo T, Isotani E, Bassel-Duby R, Williams RS: Regulation of mitochondrial biogenesis in skeletal muscle by CaMK. *Science* 296: 349–352, 2002
39. Nisoli E, Clementi E, Paolucci C, Cozzi V, Tonello C, Sciorati C, Bracale R, Valerio A, Francolini M, Moncada S, Carruba MO: Mitochondrial biogenesis in mammals: The role of endogenous nitric oxide. *Science* 299: 896–899, 2003
40. Stump CS, Short KR, Bigelow ML, Schimke JM, Nair KS: Effect of insulin on human skeletal muscle mitochondrial ATP production, protein synthesis, and mRNA transcripts. *Proc Natl Acad Sci U S A* 100: 7996–8001, 2003
41. Morrissey JJ, Ishidoya S, McCracken R, Klahr S: Nitric oxide generation ameliorates the tubulointerstitial fibrosis of obstructive nephropathy. *J Am Soc Nephrol* 7: 2202–2212, 1996
42. Li HY, Hou FF, Zhang X, Chen PY, Liu SX, Feng JX, Liu ZQ, Shan YX, Wang GB, Zhou ZM, Tian JW, Xie D: Advanced oxidation protein products accelerate renal fibrosis in a remnant kidney model. *J Am Soc Nephrol* 18: 528–538, 2007
43. Grgic I, Kiss E, Kaistha BP, Busch C, Kloss M, Sautter J, Muller A, Kaistha A, Schmidt C, Raman G, Wulff H, Strutz F, Grone HJ, Kohler R, Hoyer J: Renal fibrosis is attenuated by targeted disruption of KCa3.1 potassium channels. *Proc Natl Acad Sci U S A* 106: 14518–14523, 2009
44. Melin J, Hellberg O, Larsson E, Zezina L, Fellstrom BC: Protective effect of insulin on ischemic renal injury in diabetes mellitus. *Kidney Int* 61: 1383–1392, 2002
45. Chevalier RL, Forbes MS, Thornhill BA: Ureteral obstruction as a model of renal interstitial fibrosis and obstructive nephropathy. *Kidney Int* 75: 1145–1152, 2009
46. Chacko BK, Reily C, Srivastava A, Johnson MS, Ye Y, Ulasova E, Agarwal A, Zinn KR, Murphy MP, Kalyanaraman B, Darley-Usmar V: Prevention of diabetic nephropathy in Ins2(+/-) (AkitaJ) mice by the mitochondria-targeted therapy MitoQ. *Biochem J* 432: 9–19, 2010
47. Evans MJ, Scarpulla RC: Interaction of nuclear factors with multiple sites in the somatic cytochrome c promoter: Characterization of upstream NRF-1, ATF, and intron Sp1 recognition sequences. *J Biol Chem* 264: 14361–14368, 1989
48. Chau CM, Evans MJ, Scarpulla RC: Nuclear respiratory factor 1 activation sites in genes encoding the gamma-subunit of ATP synthase, eukaryotic initiation factor 2alpha, and tyrosine aminotransferase: Specific interaction of purified NRF-1 with multiple target genes. *J Biol Chem* 267: 6999–7006, 1992
49. Lin J, Handschin C, Spiegelman BM: Metabolic control through the PGC-1 family of transcription coactivators. *Cell Metab* 1: 361–370, 2005
50. Czubyrt MP, McAnally J, Fishman GI, Olson EN: Regulation of peroxisome proliferator-activated receptor gamma coactivator 1 alpha (PGC-1alpha) and mitochondrial function by MEF2 and HDAC5. *Proc Natl Acad Sci U S A* 100: 1711–1716, 2003
51. Rasbach KA, Green PT, Schnellmann RG: Oxidants and Ca+2 induce PGC-1alpha degradation through calpain. *Arch Biochem Biophys* 478: 130–135, 2008
52. Teyssier C, Ma H, Emter R, Kralli A, Stallcup MR: Activation of nuclear receptor coactivator PGC-1alpha by arginine methylation. *Genes Dev* 19: 1466–1473, 2005
53. Housley MP, Udeshi ND, Rodgers JT, Shabanowitz J, Puigserver P, Hunt DF, Hart GW: A PGC-1alpha-O-GlcNAc transferase complex regulates FoxO transcription factor activity in response to glucose. *J Biol Chem* 284: 5148–5157, 2009
54. Nemoto S, Fergusson MM, Finkel T: SIRT1 functionally interacts with the metabolic regulator and transcriptional coactivator PGC-1alpha. *J Biol Chem* 280: 16456–16460, 2005
55. Rodgers JT, Lerin C, Haas W, Gygi SP, Spiegelman BM, Puigserver P: Nutrient control of glucose homeostasis through a complex of PGC-1alpha and SIRT1. *Nature* 434: 113–118, 2005
56. Neutzner A, Benard G, Youle RJ, Karbowski M: Role of the ubiquitin conjugation system in the maintenance of mitochondrial homeostasis. *Ann N Y Acad Sci* 1147: 242–253, 2008
57. Wright DC, Han DH, Garcia-Roves PM, Geiger PC, Jones TE, Holloszy JO: Exercise-induced mitochondrial biogenesis begins before the increase in muscle PGC-1alpha expression. *J Biol Chem* 282: 194–199, 2007
58. Aquilano K, Vigilanza P, Baldelli S, Pagliari B, Rotilio G, Ciriolo MR: Peroxisome proliferator-activated receptor gamma co-activator 1alpha (PGC-1alpha) and sirtuin 1 (SIRT1) reside in mitochondria: possible direct function in mitochondrial biogenesis. *J Biol Chem* 285: 21590–21599, 2010
59. Arnold I, Wagner-Ecker M, Ansorge W, Langer T: Evidence for a novel mitochondria-to-nucleus signalling pathway in respiring cells lacking i-AAA protease and the ABC-transporter Mdl1. *Gene* 367: 74–88, 2006
60. Ichida M, Nemoto S, Finkel T: Identification of a specific molecular repressor of the peroxisome proliferator-activated receptor gamma coactivator-1alpha (PGC-1alpha). *J Biol Chem* 277: 50991–50995, 2002